Does the use of additional X-ray beam filtration during cine acquisition reduce clinical image quality and effective dose in cardiac interventional imaging?

Andrew G Davies[1], Amber J Gislason-Lee[1], Arnold R Cowen[1], Stephen M Kengyelics[1], Michael Lupton[2], Janet Moore[2], Mohan Sivananthan[2,]

ABSTRACT

The impact of spectral filtration in digital ("cine") acquisition was investigated using a flat panel cardiac interventional X-ray imaging system. A 0.1 mm Cu and 1.0 mm Al filter added to the standard acquisition mode created the filtered mode for comparison. Image sequences of 35 patients were acquired; a double blind subjective image quality assessment was completed and dose area product (DAP) rates were calculated. Entrance surface dose (ESD) and effective dose (E) rates were determined for 20 and 30 cm phantoms. Phantom ESD fell by 28% and 41% and E by 1% and 0.7 %, for the 20 and 30 cm phantoms respectively when using the filtration. Patient DAP rates fell by 43% with no statistically significant difference in clinical image quality. Adding 0.1 mm Cu and 1.0 mm Al filtration in acquisition substantially reduces patient ESD and DAP, with no significant change in E or clinical image quality.

INTRODUCTION

Coronary angiography and percutaneous interventional (PCI) procedures are becoming more frequent [1] in the cardiac catheterisation laboratory. Moreover, with technological medical advances there is a tendency to undertake more complex interventions, increasing the duration of imaging in these cases. There are several

reports in the literature of transient and permanent skin damage caused by cardiac catheterisation procedures [2-9], particularly with patients who require repeated coronary angiography procedures [10]. There is a need to reduce patient peak skin dose to a minimum level required for a given procedure in order to avoid these deterministic effects of radiation. In addition, stochastic effects on human tissue such as radiation-induced cancer must be avoided, in adherence with the ALARA (As Low As Reasonably Achievable) principle [11].

Cardiac X-ray systems operate in two imaging modes - fluoroscopy and digital acquisition; the latter is formerly known as 'cine' but in the context of modern digital systems the term acquisition is more appropriate and therefore used in this paper. Fluoroscopy is predominantly used to visualise interventional devices as they are manipulated inside the patient, employing a relatively low radiation dose rate. Acquisition uses higher dose rates, and commensurately provides higher fidelity imaging used for diagnosis and assessment of treatment. Although fluoroscopy dominates in terms of time, acquisition can account for over 50% of the total accrued patient procedure dose; percentages reported in the literature vary, as shown in Table 1.

Authors, Year of Publication	**Diagnostic Angiography**	**Interventional Procedures**
Betsou et al, 1998 [12]		>50%
Bakalyar et al, 1997 [13]	64%	38%
Cusma et al, 1999 [14]	70%	38%
Hummel, 2010 [15]	60%	
Efstathopoulous et al, 2004 [16]		66%
Davies et al, 2007 [17]	56-66%	

Table 1. Reported percentages of accrued patient procedure dose resulting from digital image acquisition.

In fluoroscopy, supplementary metal X-ray beam filters commonly made of copper (Cu) are used to reduce patient skin dose [18 - 26] and have also been shown to reduce staff dose [23]. Modern X-ray systems can be programmed to employ X-ray beam filters in acquisition as well as in fluoroscopy, and this has become common practice, reducing patient dose in cardiac interventions [15, 27] and neurological interventions [25]. However, the literature demonstrates concern that Cu filtration degrades angiogram image quality [21, 26]. Although the use of Cu filtration in acquisition has been investigated, its impact on clinical image quality has not been assessed [15, 24-26, 28]. It is important to assess the impact on clinical image quality of any dose saving technique. To the authors' knowledge, there are no published studies which assess clinical (i.e. patient) image quality using Cu filtration in acquisition mode for cardiac X-ray imaging.

In addition to skin dose, the stochastic, longer term effects of radiation damage should be considered in assessing the impact of X-ray beam filtration. Copper filters have been shown to increase Dose Area Product (DAP) to effective dose conversion coefficients [18, 29], leading to the preconception that using Cu filtration may lead to an undesirable increase in effective dose to the patient. Therefore the effect of Cu filtration on patient effective dose requires further investigation.

In this prospective study we investigated the effect of a Cu beam filter on patient dose - both skin dose and effective dose - in a phantom study as well as a clinical assessment of cardiac patient dose and image quality using dynamic patient image sequences.

MATERIALS AND METHODS

We assessed the effects on patient dose and image quality of introducing Cu filtration in acquisition on a modern flat panel detector X-ray system in the cardiac catheterisation laboratory at Leeds General Infirmary, UK. Modifications to an Allura XPer FD10 system (Philips Healthcare, Best, The Netherlands) were made to add an additional acquisition operating mode which was identical to the default acquisition operating mode, except that 0.1 mm Cu and 1 mm aluminium (Al) X-ray beam spectral filtration were used. The Al was used in conjunction with Cu to absorb secondary radiation generated in the primary filter [33], as is the norm for the imaging system. The default operating mode had no added spectral filtration; the total filtration of the X-ray tube not including any additional pre-filtration was 2.7 mm aluminum (Al).

Data were obtained using the default "standard" (no added filter) and the modified "filtered" (0.1 mm Cu + 1.0 mm Al filters added) acquisition modes for two separate study elements: a phantom dose study using the national standard measurement techniques [30], and a clinical study of patient dose rates and image quality using a double blinded subjective assessment. In both these study elements, results from the two different acquisition modes were compared in order to determine the effect of the added filtration on clinical image quality and patient dose.

Phantom Study

Phantom Dose

Phantom entrance surface dose (ESD) (i.e. skin dose) rates were measured using protocol outlined by the Institute of Physics and Engineering in Medicine (IPEM) working group, Martin et al [30]. A polymethylmethacrylate (PMMA) phantom was used to simulate a "standard" and "large" patient in the posterior-anterior (PA) projection, using 20 cm and 30 cm high stacks of PMMA blocks respectively, with the C-arm rotated to place the X-ray tube near the floor underneath the phantom. The PMMA blocks were placed in the X-ray beam with the table 90 cm above the floor; the authors had previously reviewed two months' worth of cardiac imaging metadata to determine this as a representative working height for PCI procedures. The phantom was raised from the surface of the patient couch by 5 cm thick wood spacers, allowing the ionisation chamber (chamber #2 shown in Figure 1) to be placed on the entrance surface of the phantom, to include backscattered radiation.

Input air kerma was also measured, in order to calculate the effective dose to the phantom. The air kerma was measured 32.5 cm in front of (below) the phantom (chamber #1 in Figure 1), and corrected for the attenuation effects of the patient table. Radcal 20X6-60 and 20X6-6 ionisation chambers with 2026C dose meters (Radcal Corp, Monrovia CA, USA), calibrated to national standards, were used to measure the phantom ESD and input air kerma respectively. Image sequences were acquired in both the standard and filtered operating modes using the 20 cm nominal (14.1 x 14.1 cm) field of view. Phantom ESD and input air kerma values were recorded once the system's automatic dose rate control (ADRC) and dose meter outputs had stabilized.

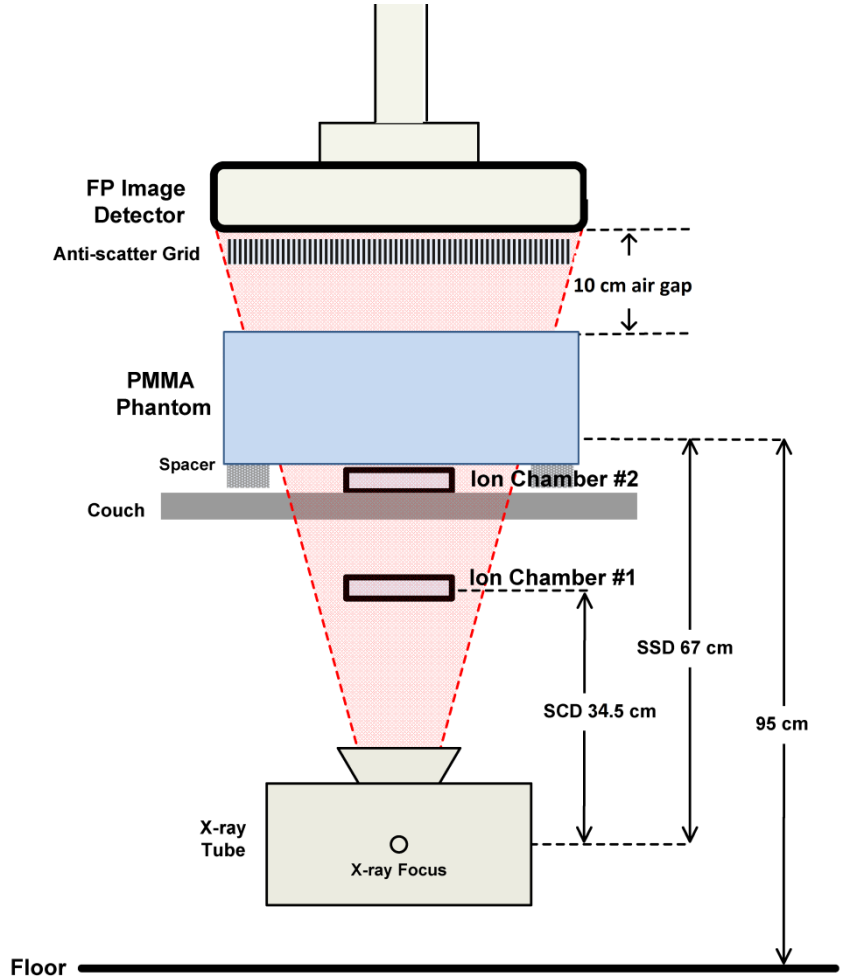

Figure 1. Experimental setup with 20 cm phantom

Imaging geometry, phantom thickness and inverse square law corrected air kerma were used to calculate effective dose rate using PCXMC software (v2.0, STUK, Finland), a computer software program which calculates effective dose rate using Monte Carlo methods and International Commission on Radiological Protection (ICRP) 103 weighting factors [34]. One million photons (the maximum amount allowed by the software) were used in the Monte Carlo simulation; this minimised the error reported by PCXMC, which was always less than 1%. Patient positioning simulated in PCXMC was the same as in the experimental setup (PA projection), so the heart, lungs, and skeleton were in the X-ray field of view. All body organ doses contributed to total effective dose. For the 20 cm phantom, the PCXMC standard height and mass were used for calculation; the patient model had a BMI of 23 kg m^{-2}.

For the 30 cm phantom, the PCXMC standard height was used and the mass was increased to 110 kg for a BMI of 34 kg m^{-2}; this adjustment, compared with the 20 cm phantom, changed the proportions of anatomy within the X-ray field of view and the distribution of radiation through the model patient.

Patient Study

Patient Dose

A group of 48 patients from those allocated to the catheterisation lab with the modified X-ray system participated in this experiment. Ethical approval was obtained from the local Research Ethics Committee, and all patients gave informed written consent to participate. The mean patient body mass index (BMI) was 29.2 ± 4.8 kg m^{-2}; this and other patient and patient procedure characteristics are shown in Table 2. Patient procedures began as usual, and the filtered acquisition mode was utilised for the remaining image sequences acquired during the patient procedure, once the clinician had established an image quality reference; standard mode image sequences acquired at the start of the procedure provided this image quality reference to ensure that image quality provided by the filtered mode was adequate and did not compromise patient care. DAP values were internally calculated and reported by the imaging system. The DAP values accrued during acquisition (i.e. excluding fluoroscopy) and corresponding numbers of image frames were recorded; using the frame rate (12.5 frames/sec), the average DAP rate per patient per acquisition operating mode was calculated.

Number of patients	48
Patient height (m)	1.69 ±0.08
Patient weight (kg)	83.9 ±16.4
Patient body mass index (BMI) (kg m^{-2})	29.2 ±4.8
Patient PA chest diameter (cm)	24.9 ±2.5
Mean number of stents per procedure [range]	1.6 ±0.9 [0 5]
Median fluoroscopy time (min) [Q1, Q3]	11.0 [7, 14.9]
Median number of frames acquired [Q1, Q3]	948 [623, 1235]
Median procedural DAP (cGy cm^2) [Q1, Q3]	3805 [2245, 5138]

Table 2. Patient and procedure details (mean ±1 standard deviation, unless otherwise stated); first and third quartiles (Q1, Q3) are shown for medians

Image Quality

Twelve months after the patient procedures were complete, four interventional cardiologist and radiologists, four X-ray radiographers, and four clinical scientists, all working in cardiology, separately compared the standard and filtered acquisition modes in a double blind study. A TG17 (Philips Healthcare, Best, The Netherlands) clinical monitor was used in a radiology viewing room where the ambient lighting conditions were dimmed, with no light source directly incident upon the monitor. No time constraints were imposed on observers for the assessment; no breaks were requested or taken.

Pairs of image sequences were created, each containing one standard and one filtered sequence from the same patient procedure, captured with matching projection angles, geometric set-up and X-ray parameters. In total 35 such pairs were created from the available patient data; for the remaining patients no match was found. Both sequences in each matching pair were displayed simultaneously on the computer monitor. This was achieved by creating a composite image sequence containing both

the standard and filtered sequences displayed side-by-side with software written in Matlab 2008a (The Mathworks, Inc, Natick, USA). This software truncated the longer of the original sequences to the length of its matching neighbour, and randomly selected which (standard or filtered) sequence was drawn on the left and which was on the right hand side of the pair, recording its selection in a key file on the host computer. This file, and thus knowledge of which sequence was the standard or filtered sequence, was not available to the observers at any stage of the experiment, nor was it available to the investigators until all viewing sessions had been completed. Images sequences were assessed by the observers choosing which of the two sequences (i.e. the left hand or right hand sequence) in the pair was preferred in terms of providing superior diagnostic image quality. Observers were also asked to state whether both images sequences in the pair had a clinically acceptable level of image quality. An example of a patient image sequence pair used in the double blind study is shown in Figure 2.

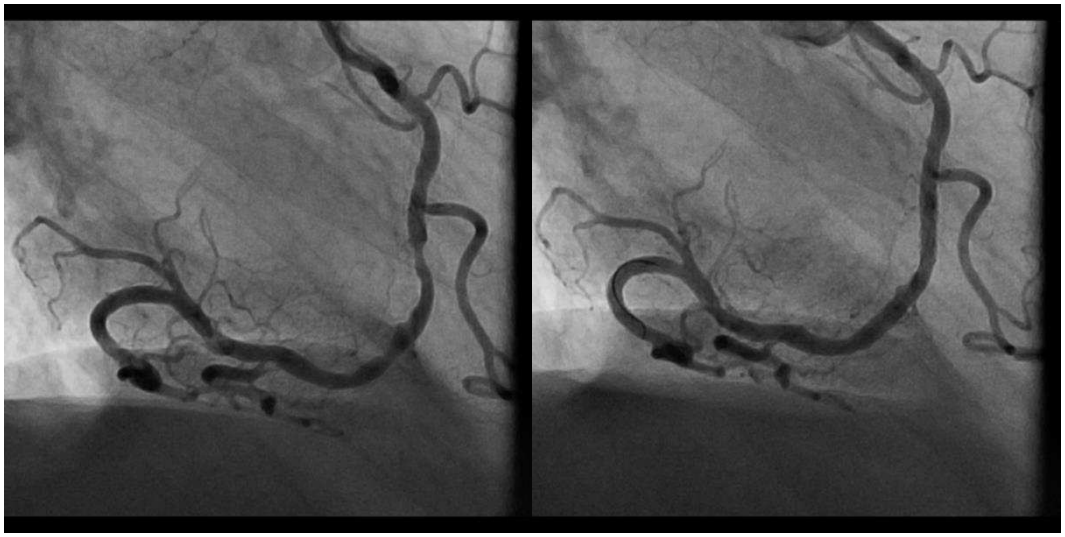

Figure 2. Standard (left) and filtered (right) mode images from the same patient for comparison

Preferred (left hand or right hand) sequences were converted to a score of -1 or +1, representing observer preference for the standard or filtered acquisition mode,

respectively, using the key file from when the sequences were created. Preferences from all the observers and all image sequence pairs were pooled and a sign test was performed to test the null hypothesis – that no difference would be found between the two different types of image sequences, standard and filtered. The sign test was single (left) tailed, and performed at the 5% significance level. The alternative hypothesis was that overall observer preference would favour the standard mode. The one-tailed test provided more power to detect an effect in one direction by not testing the effect in the other direction.

A binomial logistic regression analysis was completed in order to determine the influence of the individual observers, clinical roles, and the combination of observers and their clinical roles on subjective observations. The model was created and analysed using SPSS v16.0 (SPSS, Chicago, USA). The binomial dependent variable was the preferred (standard or filtered) image sequence. The categorical independent variables for the model were the individual observer, clinical role (interventionalist, radiographer, or clinical scientist), and combination of observer and clinical role. Pseudo R square values using the log likelihood were calculated indicating the proportion of variance in the dependent variable associated with the independent variables. The Wald statistic, which is the ratio of the logistic regression coefficient and standard error squared, was used to determine the strength of the independent variables as predictors for the dependent variable.

RESULTS

Phantom Study

Radiographic settings (i.e. acquisition parameters), X-ray tube output power and phantom dose rates are summarised in Table 3. When repeating dose measurements five times, the maximum variation in both ESD and effective dose rate was 5%. The ESD rates dropped by 28% and 40% and effective dose rates dropped by 1% and 0.7% for the 20 and 30 cm PMMA phantoms respectively when employing filtered (0.1 mm Cu + 1.0 mm Al) acquisition mode. These changes in effective dose were less than the error associated with the calculation.

	20 cm phantom		30 cm phantom	
Image Acquisition Mode	Standard	Filtered	Standard	Filtered
Peak Tube Voltage (kVp)	65	66	71	72
Tube Current (mA)	344	373	651	680
Pulse Duration (ms)	4	4	5	5
X-ray Tube Output Power (kW)	22.4	24.6	46.2	49.0
Entrance Surface Dose (μGy s^{-1}) (± 5%)	1426	1025	5460	3255
Effective Dose Rate (μSv s^{-1}) (± 5%)	9.6	9.7	18.1	18.0

Table 3. Phantom dose measurements and radiographic settings used.

Patient Study

Average patient acquisition DAP rates in the standard and filtered operating modes were 41.4 and 23.8 cGy cm^2 s^{-1} respectively; this is a reduction in patient DAP rate of 43% when switching from standard to filtered acquisition mode.

All the patient image sequences, standard and filtered mode, were deemed clinically acceptable for use in the cardiac catheterisation laboratory. There were some instances when the observers would not choose one sequence over the other,

claiming that the image quality was the same (no preference); the score was then zero. The result of the sign test on pooled scores from the twelve observers whom took part in the blind subjective image quality assessment was $p = 0.2$. The null hypothesis was therefore accepted at the 5% significance level, indicating that the observers had no preference for either the standard or filtered image sequences. Each observer's preference sums are shown in Table 4. The pseudo R square value correlating model prediction with the data was 0.021; this and the Wald statistics indicate that no independent variable in the model was significantly predictive of preference score.

Observer number	Standard mode preferred	Low dose mode preferred	No preference
1	17	18	0
2	21	14	0
3	7	8	20
4	20	11	4
5	15	14	6
6	14	12	9
7	13	12	10
8	17	18	0
9	21	14	0
10	18	17	0
11	17	18	0
12	13	22	0

Table 4. Total number of sequences preferred for each mode by each observer

DISCUSSION

Results verify past findings that a substantial reduction in patient DAP from acquisition sequences can be achieved when 0.1 mm Cu and 1.0 mm Al spectral beam filtration is employed in digital acquisition. A novel finding from this study is that with this reduction in DAP there is no significant change in subjectively assessed clinical image quality.

The hypothesis for the observer study of clinical image quality was that there would be no perceived difference between the two acquisition modes being compared, and this was accepted by the sign test. The rationale behind this hypothesis was that the change in image quality from adding the filtration would be so small that it would not be generally discernable in clinical image sequences. The authors had previously found a reduction in contrast to noise ratio (CNR) of 12% and 8% for the 20 and 30 cm PMMA phantoms respectively, using raw image data. Similarly, Fetterly [28] found a 9% decrease in CNR for water phantoms 15-40 cm thick. According to Altman's nomogram [31], the number of observations made in this study was high enough to detect a difference of 10% in preference between the two imaging modes with 80% statistical power, using a 0.05 cut-off for statistical significance, assuming each observation was independent. It is therefore highly unlikely that the result was due to chance.

An interventional X-ray system's ADRC will respond differently to different projection angles within a single patient procedure by changing the radiographic factors used. Higher patient doses generally result from steeper patient projections than shallow projections. Therefore one might be concerned that the experimental phantom setup used in this study, with only the PA projection, might not accurately represent the range of potential patient doses resulting from a cardiac catheterisation procedure. However, the reduction in DAP rate found in the patient study (using a clinically relevant range of projection angles) was found to be very similar to the reduction in ESD rate measured in the phantom study (which used one projection angle), indicating that the substantial dose savings measured in the phantom study would be realised in clinical practice.

Another novel finding is that whilst there is a reduction in ESD and/or DAP in acquisition using added filtration, the effective dose values may not change; those calculated in the phantom study using 0.1 mm Cu and 1.0 mm Al indicate no clinically significant change in effective dose due to the additional filtration. The ICRP [11] makes adjustments to tissue weighting factors used to calculate effective dose regularly, yet weighting factors for the organs of highest interest in this study are stable, with no changes made for several decades [32]; therefore there is no concern for uncertainty in these weighting factors. However, minor changes in PCXMC will change the results found in this study. For example, if a slightly thinner X-ray tube filtration was used to specify the input X-ray spectra in PCXMC, the effective dose would decrease more for the 20 cm phantom and increase slightly for the 30 cm phantom (still less than 5% differences). If the largest field of view available on the imaging system was used to calculate effective dose, with the liver and stomach in the periphery, then the effective dose would rise by about 1% for both phantom sizes. The BMI of the patient population studied was between the two BMI's used in PCXMC, so actual patient size was well represented, however effective dose strongly depends on patient size [33, 36] as well as sex. Moreover, radiographic factors selected by the ADRC impact the effective dose because they will change not only the input dose but also the penetrative characteristics of the X-ray beam. Should published conversion factors rather than PCXMC be used to calculate effective dose, these influencing factors may be reduced but results will still vary depending on the imaging system's ADRC, projection angle used, amount and type of spectral filtration, and other factors. Physicists should perform effective dose calculations using the different modes of a cardiac interventional system under various clinical scenarios in order to

assure the impact of spectral filtration on effective dose is understood for that particular system.

Patient characteristics and case complexity, duration of fluoroscopy time and number and duration of acquisition sequences varied considerably between patient procedures, resulting in a large variation in total procedural DAP between cases. This means that the reported reduction in total DAP due to the added filtration could be obscured by these confounding factors. However, the assessment of patient dose savings by using DAP rate, rather than total procedural DAP overcomes these problems by controlling for the number and length of acquisition sequences per procedure. Moreover DAP due to fluoroscopy was specifically excluded from this study.

The amount of dose reduction per patient, although expressed as DAP rate, was dependent on the thickness of the patient and also on the patient projection angles used (which may depend on the vessel of interest). However, the observers assessed intra-patient image sequence pairs, so the variation of BMI within the study will have had no impact on image quality comparisons.

No alterations to the X-ray system's ADRC programming were made, other than the introduction of the added spectral filtration, and no issues were reported relating to increased tube loading due to the filtration in the clinical cases. For the phantom study, X-ray tube output power was increased by 10% and 6% for the 20 and 30 cm phantoms respectively when the spectral filtration was added. The ADRC responded to the filtration with a modest increase of X-ray tube potential difference (by 1 kVp) for both phantom sizes.

Limitations of Study

Due to ethical considerations, use of the two acquisition modes could not be entirely randomized during patient PCI procedures. The X-ray system operator utilised the standard acquisition mode first, to ensure quality of patient care, and changed to the filtered mode once the clinician was comfortable with making the switch. The patient procedure always began with standard acquisition and ended with filtered acquisition, however the stage in the procedure when this switch occurred varied largely from patient to patient. Therefore even the investigators, upon retrospective image sequence viewing, could not estimate at which point in a patient procedure the system operator switched modes. There was no preconceived knowledge of which image sequences were captured using the standard mode and which were captured using the filtered mode, despite this limitation. This study design was advantageous in that it allowed for image sequences from the same patient to be paired for mode comparison.

The X-ray system ADRC was used during this study, as is required for safe and convenient system operation during patient procedures; radiographic factors were automatically selected by this particular system's characteristic ADRC programming. A different selection of radiographic factors would not only change the patient dose, but also impact image quality (eg. lower X-ray tube voltage increases contrast, higher tube current decreases noise). Different manufacturers, countries, and even hospitals utilize different ADRC programming techniques [34, 35], therefore results on other interventional systems may differ. Image processing settings which vary between interventional systems impact clinical image quality as well. It may be possible to further improve the performance of the imaging system, achieving a better balance

between patient dose (ESD or effective dose or both) and image quality than used in this study, for a given patient size [33, 36]. Use of sophisticated computer based image enhancement techniques or further "tuning" of the X-ray system's ADRC programming could help achieve better balance; however this study demonstrates that even without these alterations the added filtration in acquisition results in significantly lower ESD and DAP with no significant change in clinical (patient) image quality and no significant change in effective dose.

Comparison with Previous Studies

The level of dose reduction (aside from effective dose) found in this study was in broad agreement with previous studies [15, 24, 28] where a similar filter thickness was used. The current investigation focussed on the PA projection angle whereas Dragusin et al considered two completely different projection angles and a different thickness of Cu filtration [24]. Dragusin et al found an increase in effective dose with additional Cu and in the current study it remained unchanged; In addition to the projection angles being different, the ADRC in the current study increased X-ray tube voltage and current when Cu was added whereas Dragusin et al controlled X-ray settings independently, and all these factors influence effective dose. Dragusin et al used an anthropomorphic phantom for image quality assessment [24], therefore it was difficult to accurately compare dose or image quality results. However, Dragusin et al found no statistically significant impact on image quality from adding Cu filtration in acquisition mode, which is in agreement with the current study.

CONCLUSION

The impact on clinical image quality from using 0.1 mm thick copper and 1.0 mm thick aluminium spectral X-ray beam filtration in digital (cine) acquisition mode on a modern cardiac flat panel detector interventional X-ray system was investigated in a subjective assessment of dynamic patient image sequences. Observers perceived no significant change in clinical image quality with the added filtration. The same filtration provided a 43% reduction in patient acquisition DAP rate. A phantom study using PCXMC to calculate effective dose showed no clinically significant changes with the added filtration; changes were less than the error in estimation of effective dose.

The increasingly common practice of using copper X-ray beam filtration in digital acquisition has been justified in terms of patient dose (ESD and DAP) reduction, and this study has introduced its justification in terms of clinical patient image quality. This study also demonstrates that a reduction in effective dose should not be expected when using copper filtration in digital acquisition; effective dose may increase or decrease with filtration. Changes in effective dose will vary with automatic dose rate control (ADRC) programming of interventional cardiac imaging systems, as well other factors. The results from this study should not be understood as applicable to other imaging systems; physicists should conduct effective dose surveys in their interventional imaging suites.

Spectral X-ray beam filters are currently used as standard practice in fluoroscopy; where they are not yet in use for acquisition they can be programmed via manufacturer service support. This may require manufacturer assistance or an existing option may be built in for user programming, depending on the imaging system.

FUNDING

This work was supported in part by a research grant from Philips Healthcare, The Netherlands.

ACKNOWLEDGEMENTS

This study was made possible by the cooperation of radiology staff at Leeds General Infirmary's cardiac catheterization suite and by the technical support provided by Philips Healthcare, The Netherlands. Thanks to Dr Maurice Pye, Janet Waines, Lynsey Rickarson, Gershan K. Davis, Tom Bruijns, and Dr Klaus Witte for viewing the image sequence pairs.

REFERENCES

1. Faulkner, K. and Werduch, A. An estimate of the collective dose to the European population from cardiac X-ray procedures. Br J Radiol 81, 955-962 (2008).
2. Lichtenstein, D.A., Klapholz, L., Vardy, D.A., Leichter, I., Mosseri, M., Klaus, S.N. and Gilead, L.T. Chronic Radiodermatitis Following Cardiac Catheterization. Arch Dermatol 132, 663-667 (1996).
3. Dehen, L., Vilmer, C., Humiliere, C., Corcos, T., Pentousis, D., Ollivaud, L., Chatelain, D., Dubertret, L. Chronic radiodermatitis following cardiac catheterisation: a report of two cases and a brief review of the literature. Heart 81, 308-312 (1999).
4. Koenig, T.R., Mettler, F.A. and Wagner, L.K. Skin Injuries from Fluoroscopyically Guided Procedures: Part 2, Review of 73 Cases and Recommendations for Minimizing Dose Delivered to Patient. Am J Roentgenol 177, 13-20 (2000).
5. Lee, J., Hoss, D. and Phillips, T.J. Fluoroscopy-Induced Skin Necrosis. Arch Dermatol 139, 140-142 (2003).
6. Vlietstra, R.E., Wagner, L.K., Koenig, T. and Mettler, F. Radiation burns as a severe complication of fluoroscopy guided cardiological interventions. J Intervent Cardiol 17, 131-142 (2004).
7. Frazier, T.H., Richardson, J.B., Fabre, V.C. and Callen, J.P. Fluoroscopy-Induced Chronic Radiation Skin Injury A Disease Perhaps Often Overlooked. Arch Dermatol 143, 637-640 (2007).

8. Henry, M.F., Maender, J.L., Shen, Y., Tschen, J.A., Subrt, P., Schmidt J.D. and Hsu, S. Fluoroscopy-induced chronic radiation dermatitis: A report of three cases. Dermatol Online J 15(1):3 (2009).

9. Balter, S., Hopewell, J.W., Miller, D.L., Wagner, L.K. and Zelefsky, M.J. Fluoroscopically Guided Interventional Procedures: A Review of Radiation Effects on Patients' Skin and Hair. Radiology 254, 326-341 (2010).

10. Vano, E., Goicolea, J., Galvan, C., Gonzalez, L., Meiggs, L., Ten, J.I. and Macava, C. Skin radiation injuries in patients following repeated coronary angioplasty procedures. Br J Radiol. 74, 1023-1031 (2001).

11. ICRP. Recommendations of the International Commission on Radiological Protection. ICRP Publication 103. Ann ICRP 2007.

12. Betsou, S., Efstathopoulos, E.P., Datritsis, K., Faulkner, K. and Panayiotakis, G. Patient radiation doses during cardiac catheterization procedures. Br J Radiol 71, 634-639 (1998).

13. Bakalyar, D.M., Catellani, M.D. and Safian, R.D. Radiation Exposure to Patients Undergoing Diagnostic and Interventional Cardiac Catheterization Procedures. Cathet Cardiovasc Diagn 42, 121-125 (1995).

14. Cusma, J.T., Bell, M.R., Wondrow, M.A., Taubel, J.P. and Holmes, Jr D.R. Real-time measurement of radiation exposure to patients during diagnostic coronary angiography and percutaneous interventional procedures. J Am Coll Cardiol 33, 427-435 (1999).

15. Hummel, W. Comparison of KAP values for CAG examinations: the influence of parameter settings. Rad Prot Dosim 139, 363-366 (2010).

16. Efstathopoulos, E., Karvousi, S., Kottou, S., Tzanalaridou, E., Korovesis, S., Giazitzoglou, E. and Katritsis, D.G. Patient dosimetry during coronary interventions: a comprehensive analysis. Am Heart J 147, 468-475 (2004).

17. Davies, A.G., Cowen, A.R., Kengyelics, S.M., Moore, J. and Sivananthan, M.U. Do flat detector cardiac X-ray systems convey advantages over image-intensifier-based systems? Study comparing X-ray dose and image quality. Eur Radiol 17, 1787-1794 (2007).

18. Bogaert, E., Bacher, K. and Thierens, H. Interventional cardiovascular procedures in Belgium: effective dose and conversion factors Rad Prot Dosim 129, 77-82 (2008).

19. Nicholson, R., Tuffee, F. and Uthappa, C.M. Skin sparing in interventional radiology: the effect of copper filtration. Br J Radiol 73, 36-42 (2000).

20. Davies, A.G., Cowen, A., Kengyelics, S.M., Moore, J., Pepper, C., Cowan, C. and Sivananthan, M.U. X-ray Dose Reduction in Fluoroscopically Guided Electrophysiology Procedures. Pacing Clin Electrophysiol 29, 262-271 (2006).

21. ICRP. Avoidance of radiation injuries from medical interventional procedures. ICRP Publication 85. Ann ICRP 30(2), (2000).

22. Livingstone, R.S., Chandy, S., Peace, T.B.S., George, P.V., John, B. and Pati, P. Audit of radiation dose to patients during coronary angiography. Indian J Med Sci 61, 83-90 (2007).

23. den Boer, A., de Feyter, P.J., Hummel, W.A., Keane, D. and Roelandt, J.R. Reduction of radiation exposure while maintaining high-quality fluoroscopic images during interventional cardiology using novel X-ray tube technology with extra beam filtering. Circulation 89, 2710-2714 (1994).

24. Dragusin, O., Bosmans, H., Pappas, C. and Desmet, W. An investigation of flat panel equipment variables on image quality with a dedicated cardiac phantom. Phys Med Biol 53, 4927-4940 (2008).

25. Norbash, A.M., Busick, D. and Marks, M.P. Techniques for reducing interventional neuroradiologic Skin dose: tube position rotation and supplemental beam filtration. Am J Neuroradiol 17, 41-49 (1996).

26. Chida, K., Saito, H, Zuguchi, M., Shirotori, K., Kumagai, S., Nakayama, H., Matsubara, K. and Kohzuki, M. Does Digital Acquisition Reduce Patients' Skin Dose in Cardiac Interventional Procedures? Am J Roentgen 183, 1111-1114 (2004).

27. Bogaert, E., Bacher, K. and Thierens, H. A large-scale multicenter study in Belgium of dose area product values and effective doses in interventional cardiology using contemporary x-ray equipment. Rad Prot Dos 128, 312-323 (2008).

28. Fetterly, K.A. Investigation of the practical aspects of an additional 0.1 mm copper x-ray spectral filter for cine acquisition mode imaging in a clinical care setting. Health Phys 99, 624-630 (2010).

29. Smans, K., Struelens, L., Hoornaert, M.T., Bleeser, F., Buls, N., Berus, D., Clerinx, P., Malchair, F., Vanhavere, F. and Bosmans, H. A study of the correlation between dose area product and effective dose in vascular radiology. Rad Prot Dosim 130, 300-308 (2008).

30. Martin, C.J., Sutton, D.G., Workman, A., Shaw, A.J. and Temperton, D. Protocol for measurement of patient entrance surface dose rates for fluoroscopic X-ray equipment. Br J Radiol 71, 1283-1287 (1998).

31. Altman, D.G., Practical statistics for medical research. London: Chapman & Hall (1991) ISBN 0412276305.
32. ICRP, "Publication 103: Recommendations of the International Commission on Radiological Protection," Ann. ICRP (2007).
33. Gislason, A.J., Davies, A.G. and Cowen, A.R. Dose optimization in pediatric cardiac x-ray imaging. Med Phys 37, 5258-5269 (2010).
34. Lin, P.J.P., Rauch, P., Balter, S., Fukuda, A., Goode, A., Hartwell, T., LaFrance, T., Nickoloff, E., Shepard, J. and Strauss, K. Functionality and Operation of Fluoroscopic Automatic Brightness Control/Automatic Dose Rate Control Logic in Modern Cardiovascular and Interventional Angiography Systems: A Report of AAPM Task Group 125 Radiography/Fluoroscopy Subcommittee, Imaging Physics Committee, Science Council. AAPM Report No. 125, AAPM 2012.
35. Gislason, A.J., Hoornaert, B, Davies, A.G. and Cowen, A.R. Allura Xper Cardiac System Implementation of Automatic Dose Rate Control. Philips Healthcare, The Netherlands, 2011.
36. Gislason-Lee, A.J., McMillan, C., Cowen, A.R. and Davies, A.G. Dose optimization in cardiac x-ray imaging. Med Phys 40 (9), (2013).

TABLES

Table 1. Reported percentages of accrued patient procedure dose resulting from digital image acquisition.

Authors, Year of Publication	Diagnostic Angiography	Interventional Procedures
Betsou et al, 1998 [12]		>50%
Bakalyar et al, 1997 [13]	64%	38%
Cusma et al, 1999 [14]	70%	38%
Hummel, 2010 [15]	60%	
Efstathopoulous et al, 2004 [16]		66%
Davies et al, 2007 [17]	56-66%	

Table 2: Patient and procedure details (mean ±1 standard deviation, unless otherwise stated); first and third quartiles (Q1, Q3) are shown for medians.

Number of patients	48
Patient height (m)	1.69 ±0.08
Patient weight (kg)	83.9 ±16.4
Patient body mass index (BMI) (kg m^{-2})	29.2 ±4.8
Patient PA chest diameter (cm)	24.9 ±2.5
Mean number of stents per procedure [range]	1.6 ±0.9 [0 5]
Median fluoroscopy time (min) [Q1, Q3]	11.0 [7, 14.9]
Median number of frames acquired [Q1, Q3]	948 [623, 1235]
Median procedural DAP (cGy cm^2) [Q1, Q3]	3805 [2245, 5138]

Table 3. Phantom dose measurements and radiographic settings used.

	20 cm phantom		30 cm phantom	
Image Acquisition Mode	Standard	Filtered	Standard	Filtered
Peak Tube Voltage (kVp)	65	66	71	72
Tube Current (mA)	344	373	651	680
Pulse Duration (ms)	4	4	5	5
X-ray Tube Output Power (kW)	22.4	24.6	46.2	49.0
Entrance Surface Dose (μGy s^{-1}) (± 5%)	1426	1025	5460	3255
Effective Dose Rate (μSv s^{-1}) (± 5%)	9.6	9.7	18.1	18.0

Table 4. Total number of sequences preferred for each mode by each observer.

Observer number	Standard mode preferred	Low dose mode preferred	No preference
1	17	18	0
2	21	14	0
3	7	8	20
4	20	11	4
5	15	14	6
6	14	12	9
7	13	12	10
8	17	18	0
9	21	14	0
10	18	17	0
11	17	18	0
12	13	22	0

FIGURE LEGENDS

Figure 1. Experimental setup with 20 cm phantom

Figure 2. Standard (a) and filtered (b) mode images from the same patient for comparison